

Elastic magnetic scattering of electrons from ^{13}C

R. S. Hicks, J. Dubach, R. A. Lindgren, B. Parker, and G. A. Peterson

*Department of Physics and Astronomy, University of Massachusetts,**Amherst, Massachusetts 01003*

(Received 23 March 1982)

The form factor for elastic magnetic scattering of electrons from ^{13}C has been measured to a maximum momentum transfer of 3.29 fm^{-1} . No reasonable p -shell model, with or without one-pion exchange currents, could be found to explain the relative enhancement observed in the $M1$ form factor above $q \approx 2 \text{ fm}^{-1}$.

[NUCLEAR REACTIONS $^{13}\text{C}(e, e)$, $E = 80\text{--}338 \text{ MeV}$; measured] $\sigma(E, \theta)$. ^{13}C deduced $M1$ form factor. Comparison with shell model.]

I. INTRODUCTION

Many of the observable properties of nuclei are strongly determined by the particles in the outermost shell-model orbitals. In non-zero-spin nuclei, the magnetic elastic scattering of electrons provides a sensitive and direct means of studying these orbits. For example, consider the case of $M1$ multipole scattering from a $1p$ -shell nucleus of assumed configuration space $(1s)^4(1p)^{A-4}$. In this model the (e, e) $M1$ form factor may be written^{1,2}

$$F_{M1}(q) \sim q\mu [\langle 1p || j_0(qr) || 1p \rangle - \alpha \langle 1p || j_2(qr) || 1p \rangle], \quad (1a)$$

where q is the momentum transfer, r is the nuclear radial coordinate, j_0 and j_2 are spherical Bessel functions, and μ is the nuclear dipole moment. The coefficient α depends upon details of nuclear structure and strongly influences the q dependence of the $M1$ form factor. This may be easily demonstrated by choosing harmonic oscillator single-particle wave functions, in which case the above expression reduces to the simple form¹

$$F_{M1}(q) \sim q\mu [1 - \frac{2}{3}(1 + \alpha)x] e^{-x}, \quad (1b)$$

where the parameter x is defined in terms of the oscillator size parameter b :

$$x = \left[\frac{bq}{2} \right]^2.$$

Equation (1b) predicts that the $M1$ form factor will possess only two diffraction zeros, one at $q=0$ and a second at

$$q_{\min} = \frac{1}{b} \left[\frac{6}{(q + \alpha)} \right]^{1/2}.$$

For the particular case of ^{13}C , various model calculations give α as 2.00 (jj coupling or extreme single particle), 0.29 (LS coupling), and 1.20 (Cohen-Kurath shell model coupling).² Accordingly, the second diffraction minimum may be expected to lie between $q = 1.41/b$ and $2.16/b$. Careful (e, e) measurements would be expected to locate this minimum within an accuracy of better than 0.1 fm^{-1} , and thereby impose a strong constraint on the configuration of the valence p -shell nucleons.

By way of comparison, the determination of ground state charge distributions by the elastic scattering of electrons is rather insensitive to the valence orbital structure. In this case, the contribution of the p -shell nucleons enters only by the $\langle 1p || j_0 || 1p \rangle$ single-particle matrix element, and thus does not provide the opportunity to measure structure-dependent cancellation effects as in magnetic scattering. The insensitivity of elastic charge scattering to the configuration of the valence nucleons is especially apparent for nuclei whose structure is largely determined by an unpaired neutron. To some extent, the comparison of elastic charge scattering from adjacent isotopes can provide indirect information about the role played by a valence neutron: We may investigate how the unpaired neutron polarizes the even- A "core." However, it remains that one of the most direct and stringent tests of the structure of the valence orbitals is provided by elastic magnetic scattering.

Recent theoretical studies have, however, led to suggestions that the zeroth-order p -shell picture, represented by Eq. (1a), at best provides only a crude approximation to the observed (e, e') form factor. For example, it has been proposed that there may be significant contributions from outside the $1p$ -shell, nuclear structure effects frequently

described as “core polarization.”^{3,4} Moreover, detailed evaluations⁵ of one-pion exchange currents have predicted 20–100% effects over much of the q range of $M1$ form factors. Precursors to pion condensation have also been proposed.^{6–8} Despite claims that such effects might contribute strongly to isovector $M1$ form factors, recent (p, p') measurements^{9,10} of the 15.1 MeV transition in ^{12}C find little evidence to support such a conclusion. Other mesonic processes of suggested importance, especially in the high- q domain, are two-pion and rho-meson exchanges.

In light of these proposals, the extent to which the electron scattering data can be utilized to precisely define the underlying p -shell structure of $M1$ -excited states is perhaps questionable. In fact, as we shall see, the simple p -shell picture seems fundamentally incapable of explaining the measured ^{13}C $M1$ form factor above 2.3 fm^{-1} . Similar results have been found for other p -shell $M1$ form factors. These discrepancies have stimulated renewed interest in the possible role of meson degrees of freedom in finite nuclei.

It should be clear that to adequately scrutinize the proposed theories, extensive and systematic data are required on a number of $M1$ transitions. To meet this need, and to explore basic structure questions, we have measured the elastic $M1$ cross section for the nucleus ^{13}C . The $J^\pi = \frac{1}{2}^-$ ground-state spin of ^{13}C ensures that the transverse interaction proceeds only by the $M1$ multipole, and thus no model-dependent subtraction of $M3$ or higher magnetic multipole is required. Also, because ^{13}C is an odd- A nucleus, the dominantly isovector exchange currents should contribute more strongly than in the case of a purely isoscalar transition.

II. EXPERIMENTAL DETAILS

The experiment was performed by using the electron scattering facility¹¹ of the Bates Linear Accelerator in Middleton, Massachusetts. Data were collected primarily at a scattering angle of 180° , using a four-magnet system¹² to deflect back-scattered electrons into a 900 MeV/ c magnetic spectrometer. Incident electron energies ranged from 80–338 MeV, corresponding to momentum transfers between 0.8 and 3.29 fm^{-1} . Two of the high- q data points were measured at a scattering angle of 160° .

The target consisted of graphite powder enriched to 93% in ^{13}C and contained in an aluminum frame between two natural carbon foils, each of thickness 15 mg/cm^2 . Constructional details of this target

are in other respects similar to that of a ^{14}C target described by Kline *et al.*¹³ The final composition and thickness of the ^{13}C target was established by conducting measurements at a scattering angle of 90° , where a comparison could be made against the precisely-known Coulomb cross sections of ^{12}C . The target thickness thus determined was $147.4 \pm 2.0 \text{ mg/cm}^2$ for ^{13}C and $39.3 \pm 0.4 \text{ mg/cm}^2$ for ^{12}C , averaged over the central region of the target irradiated by the dispersed beam spot.¹¹

As backward scattering angles are approached, the Coulomb contribution to the total elastic cross section decreases sharply. Nevertheless, even at 180° , Coulomb contamination in the measured cross sections can be appreciable. This arises from the combined effects of the finite angular acceptance of the spectrometer, multiple scattering within the target, and the nonzero electron rest mass.^{14,15} Figure 1 shows the ratio of the transverse $M1$ to total (transverse $M1$ plus Coulomb C0) cross sections for ^{13}C under various experimental conditions. Consider first scattering through an angle of 165° , which is about the maximum deflection one can measure without the use of a specialized magnet system. For momentum transfers below 1.4 fm^{-1} , $M1$ scattering events constitute less than 10% of the to-

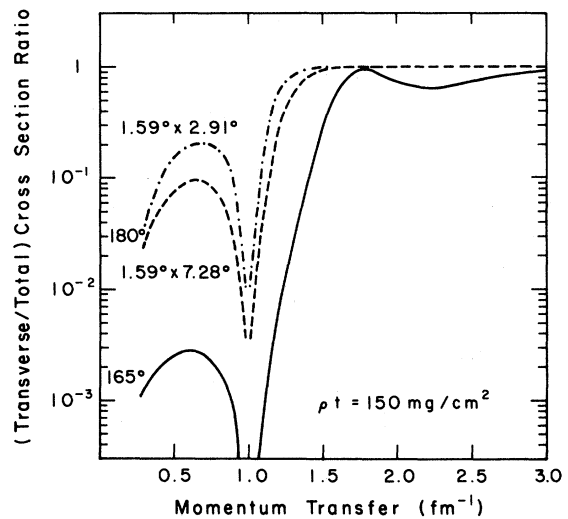


FIG. 1. Ratio of transverse $M1$ to total (transverse $M1$ plus longitudinal C0) cross sections for elastic scattering of electrons from ^{13}C at angles of 165° and 180° . The two 180° curves correspond to spectrometer acceptance angles of 1.41 msr ($1.56^\circ \times 2.91^\circ$) and 3.53 msr ($1.59^\circ \times 7.28^\circ$). $M1$ and C0 cross section minima occur at 1.0 and 1.8 fm^{-1} . Multiple-scattering effects were calculated for an assumed target thickness of 150 mg/cm^2 .

the total recorded counts. At this angle, measurement of the $M1$ cross section only becomes feasible above $q \simeq 1.5 \text{ fm}^{-1}$, and even at 2.3 fm^{-1} , one-third of the accumulated counts originate from Coulomb interactions. The dashed and dotted-dashed curves show the corresponding cross section ratio for 180° scattering with two different spectrometer acceptance solid angles. The angles denote the full angular ranges subtended at the target by the rectangular spectrometer aperture. For $q < 1.5 \text{ fm}^{-1}$, 180° scattering claims a two order-of-magnitude advantage in signal-to-background ratio over 165° scattering. Yet, even for scattering at 180° with a restricted angular acceptance, it is seen that the transverse events account for only 10–20% of the total recorded counts in the region of the first $M1$ diffraction maximum ($q \simeq 0.4\text{--}0.9 \text{ fm}^{-1}$).

Extensive measurements of the first $M1$ diffraction maximum have been made by the Amsterdam group.² It is a tribute to these workers that they were able to reliably separate the meagre $M1$ cross section from the dominant Coulomb component. The method for subtracting the Coulomb contribution rests upon the additional measurement of purely Coulomb scattering from a neighboring spin-zero nucleus. For this purpose, we utilized a natural carbon foil, making allowance for the 1.11% ^{13}C abundance in natural carbon. Since the ^{13}C and ^{12}C charge densities are well known,¹⁶ the ratio of the 180° Coulomb cross sections can then be calculated in distorted-wave Born approximation, enabling the measured data to be finally corrected for charge scattering.

In the $q \simeq 1.0 \text{ fm}^{-1}$ diffraction minimum of the ^{13}C $M1$ form factor charge subtractions exceeded 90% of the total measured cross section. Careful forethought to the setting of the spectrometer acceptance solid angle $\Delta\Omega$ can help facilitate such difficult measurements. Near 180° the measured differential transverse cross section $d\sigma_T/d\Omega$ is approximately independent of $\Delta\Omega$, whereas the corresponding Coulomb cross section $d\sigma_C/d\Omega$ increases quadratically with the opening of the spectrometer aperture.^{14,15} Therefore, as $\Delta\Omega$ is increased proportionately more Coulomb-scattered electrons are counted by electron detectors. On the other hand, if we were to close down the spectrometer slits to improve the (transverse) signal-to-(Coulomb) background ratio, the already low transverse count rate would be diminished further. Clearly there exists some intermediate acceptance solid angle for which the best possible precision can be obtained within a fixed measurement time interval.

During the course of an experiment it often be-

comes possible to estimate in advance the values of still-to-be-measured data points by the interpolation of earlier measurements. Also, using known charge densities the absolute Coulomb background count rate at 180° can be predicted within an uncertainty of about 35%.¹² We utilize this information to compute the optimum spectrometer aperture setting prior to the measurement of a particular data point.¹⁷ Simultaneously the most efficient division of available experimental time between the studied target and the Coulomb background target is also determined. Nevertheless, the measurement of small $M1$ cross sections in the presence of an overwhelming Coulomb background is still a time-consuming task. Despite a $40 \mu\text{A}$ incident electron beam and a thick (147.4 mg/cm^2) target, the measurement of individual data points near the ^{13}C $M1$ diffraction minimum required in excess of 4 h of beam time. Further discussion of aspects of the Coulomb subtraction procedure may be found in Refs. 2, 14, and 18.

III. ANALYSIS OF DATA

The data were analyzed according to procedures described elsewhere.¹⁹ Correct absolute normalization of the results was ensured by making additional measurements of the proton elastic cross section, which is well known.²⁰ For presentation of the results we have transformed the measured cross sections into transverse form factors using

$$\frac{d\sigma_T}{d\Omega}(k_1, \theta = 180^\circ) = \left[\frac{Z\alpha\hbar}{2k_1} \right]^2 \left[1 + \frac{2k_1}{Mc} \right]^{-1} \times F_{M1}^2(q), \quad (2)$$

where k_1 is the incident electron momentum and M is the nuclear mass. In this particular normalization the corresponding elastic C0 form factor would approach unity at $q \rightarrow 0$.

Equation (2), the plane-wave Born approximation result, is only useful to the extent that Coulomb distortion effects can be neglected. The ^{13}C results presented in Table I have been corrected for Coulomb distortion using an iterative procedure in which the experimental data were first least-squares fitted with a polynomial expression of the type²¹

$$F_{M1}(q) = \frac{1}{\sqrt{2}} \left[\frac{\mu\hbar c}{ZM_N} \right] qe^{-x} \times (1 + a_1x + a_2x^2 + a_3x^3) f_{\text{SN}} f_{\text{CM}}, \quad (3)$$

where M_N is the nucleon mass and f_{SN} and f_{CM}

TABLE I. $M1$ form factor results deduced from experimental measurements at 180° and 160° ($k_1 = 258.87$ and 337.87 MeV/ c). Plane-wave form factors may be obtained by multiplying the tabulated values by the corresponding distortion-correction factors f . The results of Lapikas *et al.* (Ref. 2) are included for completeness.

k_1 (MeV/ c)	q (fm^{-1})	F_{M1}^2 ($\times 10^6$)	$\sigma(F_{M1}^2)$ (%)	f
Amsterdam results [Lapikas <i>et al.</i> (Ref. 2)]				
40.00	0.404	34.0	11.4	0.912
45.00	0.454	32.7	9.7	0.930
50.00	0.505	27.6	9.8	0.950
55.00	0.555	30.1	9.8	0.973
60.00	0.605	25.3	8.5	1.001
65.00	0.655	18.5	9.9	1.032
70.00	0.705	15.1	12.3	1.071
75.00	0.756	11.9	12.8	1.129
80.00	0.806	9.40	22.2	1.207
85.00	0.856	5.50	28.6	1.331
90.00	0.906	2.64	66.7	1.572
Bates results				
80.55	0.811	11.1	21.7	1.215
89.97	0.905	2.92	47.5	1.563
100.87	1.014	2.58	418.0	2.780
109.50	1.100	1.71	39.5	0.362
120.55	1.210	7.69	11.5	0.662
130.40	1.308	10.4	7.3	0.772
139.70	1.400	14.2	6.8	0.834
150.75	1.509	17.3	6.9	0.891
165.84	1.658	17.9	5.6	0.952
179.79	1.796	19.0	6.0	0.987
193.36	1.929	17.9	5.9	1.017
199.42	1.989	17.0	10.1	1.026
209.90	2.092	14.2	6.0	1.039
223.98	2.230	12.1	6.1	1.054
238.07	2.367	9.59	6.2	1.063
258.87	2.532	6.84	7.9	1.070
278.70	2.763	4.65	10.5	1.108
298.77	2.957	2.81	10.2	1.146
319.79	3.160	1.38	13.7	1.190
337.87	3.286	0.85	16.2	1.240

are the single-nucleon and shell model center-of-mass corrections.²¹ The fitted form factor was then transformed into a corresponding magnetization density, enabling distortion correction factors to be computed using a DWBA code.²² The first-iteration distortion-corrected data were subsequently refitted, and the entire procedure repeated until convergence was obtained.

For comparison with theoretical calculations the present results have been combined with the low- q data of Lapikas *et al.*,² providing comprehensive coverage of the entire region between $q = 0.40$ and 3.29 fm^{-1} . Additional data points were obtained by Heisenberg *et al.*²³ by Rosenbluth separation in the

vicinity of the first diffraction minimum of the charge form factor. These measurements, clustered around 2 fm^{-1} , lie in good agreement with the present results and hence have not been utilized for the theoretical comparisons.

IV. $1p$ -SHELL INTERPRETATION

In this section we will endeavor to account for the measured $M1$ form factor in terms of $0\hbar\omega$ p -shell nuclear structure, with and without one-pion exchange currents. In the calculation of shell-model (e, e) form factors it is necessary to adopt a

length parameter to set the scale of the radial wave functions, usually derived from harmonic oscillator or Woods-Saxon potentials. To account for magnetic scattering data some authors have used radial parameters deduced from elastic charge scattering. This procedure is questionable, since as discussed earlier, magnetic and charge scattering experiments probe different aspects of the nuclear ground state structure.²⁴ We anticipate that the $M1$ form factor of ^{13}C will be primarily determined by nucleons in the $1p_{1/2}$ and $1p_{3/2}$ orbits. Using Hartree-Fock methods, Quentin²⁵ has evaluated the corresponding equivalent oscillator size parameters as $b_{1/2}=1.83$ fm and $b_{3/2}=1.65$ fm. (The "average" oscillator parameter deduced from the measured rms charge radius is 1.61 ± 0.01 fm.) Reliable experimental information on the radial size of individual orbits is lacking at the present time. In the absence of such data we have adopted a procedure in which all orbits share a common radial parameter chosen to locate the ^{13}C $M1$ diffraction minimum at the observed value of $q=1.04$ fm $^{-1}$. The derived radial scale parameter thus represents an average over the contributing orbitals, weighted according to each particular model.

The first comparison, shown in Fig. 2(a), is with the predictions of three p -shell models, calculated using harmonic oscillator wave functions. The LS -coupling model greatly overestimates the magnitude of the first diffraction maximum. Inspection of Eq. (1b) shows that this discrepancy is not unexpected since the LS -coupling model predicts a dipole moment of $1.10 \mu_N$,²⁶ a value in considerable excess of the observed moment of $0.7024 \mu_N$. The moments given by the jj -coupling model (equivalent to the extreme single-particle description) and the Cohen-Kurath model²⁶ [(8-16) 2BME], 0.64 and $0.70 \mu_N$, are seen to lie in better agreement with the experimental result. However, in order to correctly locate the $M1$ diffraction minimum at $q=1.04$ fm $^{-1}$, the jj -coupling description requires an oscillator parameter of $b=1.36$ fm. We consider this value implausible for ^{13}C . Only the Cohen-Kurath model provides an acceptable fit to the first diffraction maximum with a reasonable oscillator parameter ($b=1.59$ fm). However, the most striking aspect of the comparison shown in Fig. 2(a) is the complete failure of all three calculations to account for the experimental data in the region surrounding the second diffraction maximum. In particular, one notes a marked relative enhancement of the high- q data, leading to a decreased slope above $q\approx 2$ fm $^{-1}$ which none of the model calculations can reproduce.

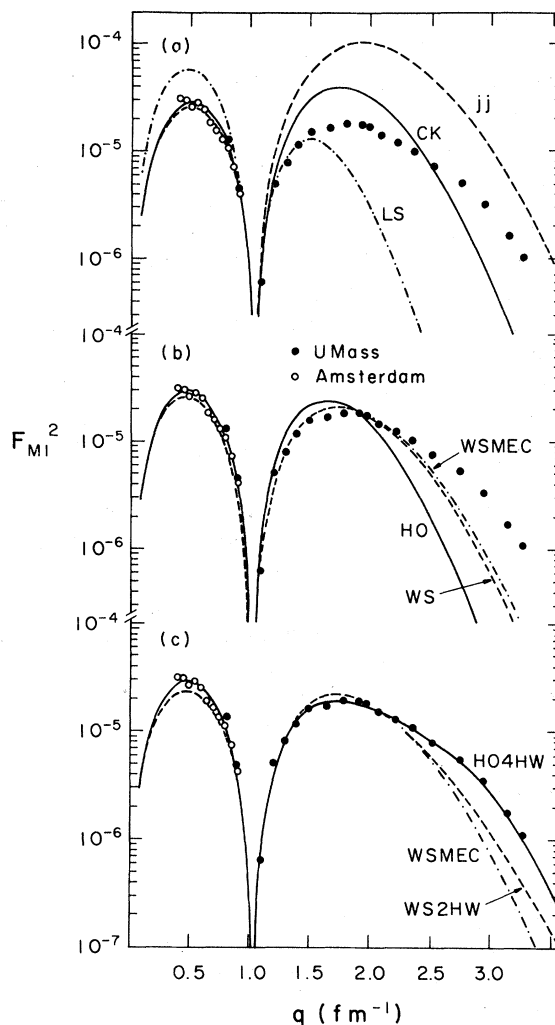


FIG. 2. Transverse form factor data and comparison with p -shell interpretations. The results of the present measurements are indicated by solid circles; open circles represent the data of Lapikas *et al.* (Ref. 2). All data have been corrected for Coulomb distortion effects as described in the text. (a) Comparison with LS coupling, jj coupling, and the Cohen-Kurath (Ref. 26) model. Respective oscillator size parameters of 2.07, 1.36, and 1.59 fm are required to locate the diffraction minimum at 1.04 fm $^{-1}$. (b) Results of attempts to fit the data with a generalized p -shell model. HO, harmonic oscillator, $b=1.73$ fm and $\alpha=0.85$; WS, Woods-Saxon, $R_0=1.17$ fm and $\alpha=0.48$; WSMEC, Woods-Saxon including one-pion exchange, $R_0=1.24$ fm and $\alpha=0.31$. All calculations reproduce the measured dipole magnetic moment. (c) Phenomenological evaluation of possible core polarization contributions. WSMEC, same as in (b); HO4HW, $4\hbar\omega$ harmonic oscillator fit, $b=1.61$ fm; WS2HW, fit including $2\hbar\omega$ ($2p_{1/2}1p_{1/2}^{-1}$) $_v$ matrix element calculated using Woods-Saxon wave functions. All curves include one-pion exchange current contributions evaluated for the $1p$ shell only.

The failure of these simple models leads to the study of less restrictive p -shell models in which the coupling coefficient α is left as an adjustable parameter. The harmonic oscillator (HO) curve in Fig. 2(b) shows the result of performing such a fit to the data using harmonic oscillator wave functions. The best-fit result, constrained to the experimentally determined dipole moment, corresponds to $\alpha=0.85$ and $b=1.73$ fm. It is immediately apparent that no p -shell, harmonic oscillator model can account for the observed data over the entire q range.

Since the measurements span an extended range of momentum transfer, some sensitivity to the form of the radial wave functions will be exhibited. Harmonic oscillator wave functions are known to seriously underestimate the densities of $1p$ orbitals for $r > 4$ fm.²⁷ Accordingly, the analysis was repeated using more realistic wave functions derived from a Woods-Saxon potential. For this calculation, the diffuseness parameter was taken to be 0.5 fm, and the well depth chosen to reproduce the observed neutron separation energy of 4.95 MeV. Center-of-mass and nucleon size corrections²⁸ were included in the same factorable form that is employed for harmonic oscillator calculations. For simplicity, the spin-orbit and Coulomb terms were neglected. The best-fit result, indicated by the Woods-Saxon (WS) curve in Fig. 2(b), shows a clear improvement over the harmonic oscillator description but still lies one order of magnitude below the data at high q . The coupling coefficient found was $\alpha=0.48$, with a value of $R_0=1.17$ fm being obtained for the Woods-Saxon radial parameter.

In a further attempt to describe the data, specific consideration was given to meson exchange currents, computed using the two-body density matrix derived from the Cohen-Kurath interaction. For ease of calculation we have evaluated the pair, pionic, and nucleon resonance⁵ terms using harmonic oscillator wave functions with $b=1.70$ fm. The calculated one-pion exchange currents have a q dependence very similar to the one-body currents and, as shown in Fig. 3, provide a 20% enhancement over the Cohen-Kurath prediction at the second maximum of the ^{13}C form factor. Nevertheless, refitting the data leads to a curve (WSMEC), which shows little improvement over the fit obtained without exchange currents. Note, however, that in order to accommodate the appreciable exchange current contributions, the one-body structure undergoes a sizeable readjustment, as reflected in the revised values obtained for the p -shell coupling coefficient and the Woods-Saxon radius

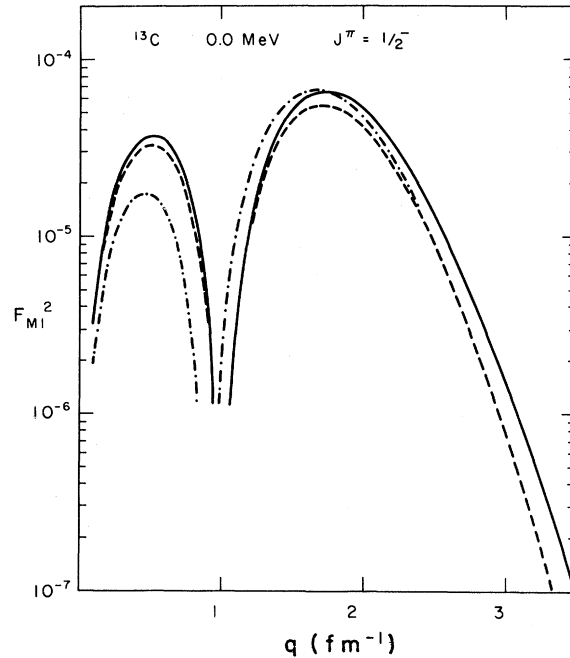


FIG. 3. Spherical-basis $2\hbar\omega$ shell-model predictions for the ^{13}C magnetic form factor, calculated using harmonic oscillator wave functions ($b=1.60$ fm). Dotted-dashed curve, intrinsic magnetization currents only; dashed curve, magnetization and convection currents; continuous curve, magnetization, convection, and one-pion exchange currents. The exchange current contribution was computed with an oscillator size parameter of $b=1.70$ fm.

parameter, $\alpha=0.31$ and $R_0=1.24$ fm. A similar observation was reported by Dubach and Haxton⁵ in their analysis of the ^{12}C 15.1 MeV form factor.

A possible weakness in these attempted interpretations may be the use of a nucleon finite size correction that is adopted from the results of measurements on the proton and deuteron. Field-theoretic treatments²⁹ have predicted an appreciable mesonic renormalization of the nucleon's properties when it is the constituent of a nucleus in which the forces are close to saturation. In particular, the consideration of quasielastic electron scattering led Noble²⁹ to suggest that the nucleon's size might be about 30% larger in nuclear matter. Such an increase would strongly influence the behavior of (e,e) form factors at high q . This idea may be examined by varying the nucleon size parameter in the single nucleon form factor f_{SN} . Application of this procedure to the present case, using the form³⁰

$$f_{\text{SN}}(q) = \exp(-a_p^2 q^2 / 4),$$

leads to a result which shows little improvement in the overall quality of fit. Moreover, the best-fit value of the nucleon size parameter, $a_p = 0.65 \pm 0.01$ fm, lies in good agreement with the value measured for the charge radius of the bare proton.

Thus the assumption of a larger nucleon size cannot resolve the problem encountered in the explanation of the data at high q . It has been seen how this difficulty has persisted in spite of the inclusion of one-pion exchange currents, the use of realistic radial wave functions, and the assignment of complete freedom to the p -shell coupling.

V. MULTI- $\hbar\omega$ CONFIGURATIONS

In order to evaluate the possible role of higher order shell-model components in the ground state, we have used the results of a preliminary calculation for ^{13}C performed in a full $2\hbar\omega$ configuration space by Dubach and Haxton.³¹ These calculations emphasized the $2\hbar\omega$ configurations with two particles in the sd shell. Configurations with a noninteracting particle in the pf shell, or noninteracting hole in the ^4He core, were included only to enable the complete elimination of spurious center-of-mass excitations. The inclusion of the $2\hbar\omega$ admixtures had only a minor effect on the elastic form factor. Compared to the Cohen-Kurath prediction, a 9% increase was realized at the first form factor diffraction maximum, with smaller effects in the vicinity of the second maximum, at least as far as 3.5 fm^{-1} .

On the other hand, core polarization calculations by Suzuki *et al.*⁴ and others^{7,8} indicate that multi- $\hbar\omega$ single particle-hole excitations make sizable contributions. For example, the $12\hbar\omega$ calculation of Suzuki *et al.*⁴ shows a strong destructive interference between the core polarization component and the p -shell and two-body terms at the second diffraction maximum. This reduces the Cohen-Kurath prediction by about a factor of 3 at $q = 1.8 \text{ fm}^{-1}$. At $q = 3.0 \text{ fm}^{-1}$, however, the core polarization contribution enhances the form factor so that the final comparison with the experimental result shows improved, albeit not complete, agreement. Applied to the 15.1 MeV $M1$ transition in ^{12}C , a similar calculation leads to a less satisfactory result,⁴ for the predictions already lie an order of magnitude too low at $q = 2.6 \text{ fm}^{-1}$. In general, about half of the core polarization effect computed by Suzuki is attributed to $2\hbar\omega$ configurations.³²

Some insight into the role of core polarization may be developed by least-square fitting the exchange-current-corrected ^{13}C data with the general polynomial expression shown in Eq. (3). In the simplest harmonic oscillator p -shell space, only terms up to the order of x^1 are retained. Each successive power of x admitted implies an additional $2\hbar\omega$ increase in the oscillator configuration space. As has been already demonstrated, the data are poorly fit if the polynomial is constrained to be linear in x . Little improvement is realized in the χ^2 value by the introduction of the quadratic term. However, when the term cubic in x is included, a near-perfect fit is obtained, corresponding to the fitted parameters $b = 1.61 \pm 0.02$, $a_1 = -0.179 \pm 0.005$, $a_2 = 0.063 \pm 0.004$, and $a_3 = -0.013 \pm 0.001$. The result, indicated in Fig. 2(c) by the notation HO4HW, suggests a sizable admixture of $4\hbar\omega$ configurations in the ^{13}C ground state.

On the other hand, in view of the importance previously attached to the use of realistic radial wave functions, one may question the validity of the harmonic oscillator interpretation derived from the low-order polynomial analysis. In order to assess possible radial wave function effects we have performed a similar analysis using Woods-Saxon wave functions. The first step in this procedure was to search for a $2\hbar\omega$ single-particle matrix element that could provide a large enhancement at high q , without significantly affecting the fit at low momentum transfers. The most plausible candidate was found to be the $(2p_{1/2}, 1p_{1/2}^{-1})$ neutron matrix element, which we calculated using the Woods-Saxon well parameters previously established. The amplitudes of the $0\hbar\omega$ and $2\hbar\omega$ terms were then varied to find the best fit to the data, subject to the usual constraints of correctly reproducing the measured dipole moment as well as the observed diffraction minimum at $q = 1.04 \text{ fm}^{-1}$. The result, denoted in Fig. 2(c) by the label WS2HW, includes a $(2p_{1/2}, 1p_{1/2}^{-1})_v$ admixture equal to 16% of the full particle-hole matrix element. Although the inclusion of this $2\hbar\omega$ matrix element provides a noticeable improvement over the $0\hbar\omega$ description, it is unclear whether the remaining high- q discrepancy can be accounted for by a more complete treatment of the $2\hbar\omega$ admixtures.

Although the development of a valid procedure for assessing core polarization effects is of obvious importance, the reliability of many existing evaluations is uncertain. The consistency of these procedures should be checked for cases where core polarization represents the dominant term, and not a second-order effect, as is the case for magnetic

scattering. A more apposite choice would be to study the static charge properties of states or transitions whose character is primarily determined by an unpaired neutron. One could, for example, evaluate the quadrupole moment of the $J^\pi = \frac{5}{2}^+$ ground state of ^{17}O , or the $C2$ form factor for the $\frac{1}{2}^+$ state at 0.87 MeV.³³ Further examples are the ratios of the Coulomb (e, e) form factors for ^{17}O and ^{16}O (Ref. 34), or ^{13}C and ^{12}C . Such properties are often poorly described by shell model calculations that do not employ effective charges. An additional advantage of this type of investigation is that the uncertain meson exchange terms are expected to contribute only weakly, and so the comparison between theory and experiment should be rather direct.

In an attempt to construct a model that reflects more explicitly the large deformations of the isotopes, Lin and Zamick³⁵ have performed calculations using Nilsson model wave functions for a $p_{1/2}$ neutron outside a $s_{1/2}^4 p_{3/2}^8$ core. Following the introduction of $2\hbar\omega$ admixtures into the Nilsson model wave functions, they obtain a result quantitatively very similar to the form factor predicted by the spherical basis shell-model calculations. Near equivalence of the two procedures may not be unexpected. As Kurath and Picman³⁶ have pointed out, since the eigenfunctions of a deformed Hamiltonian can be expanded as sums of isotropic wave functions, essentially complete overlap can exist between wave functions generated in deformed and spherical potentials if the model space is sufficiently large. As an example of the possible equivalence between the two approaches, we have indicated in Fig. 3 how the spherical-basis convection currents enhance the $M1$ form factor as far as the second diffraction maximum. A very similar result is given by the

Nilsson model.³⁵ Of course, one advantage of the Nilsson model is that it provides a more easily appreciated physical picture of the deformed wave function of the $p_{1/2}$ neutron than does the spherical-basis model with its strongly mixed configurations.

VI. SUMMARY

We have been unable to find a fundamental model capable of accurately describing the ^{13}C elastic data over the entire measured range in q . The most serious difficulty is the large relative enhancement of the data beyond the second diffraction maximum. In particular, no reasonable p -shell model, with or without one-pion exchange currents, is able to account for this effect. It has been suggested that mesonic interactions of shorter range than one-pion exchange may be responsible. Two-pion exchange, Δ -intermediate states, and rho meson exchange have been proposed as likely candidates.⁶⁻⁸ Unfortunately, existing evaluations of these processes are embedded in possibly inappropriate core polarization formalism.⁴ Whether or not the high- q enhancements observed^{27,37} in ^{13}C , ^{12}C , ^6Li , and other $M1$ form factors³⁸ is attributable to incompletely understood mesonic processes, or to other more "conventional" effects such as clustering³⁹ or, in contradistinction to shell-model assumptions, a highly polarized core, remains to be seen.

This work was funded in part by the U.S. Department of Energy under contracts with the Bates Linear Accelerator Laboratory and the University of Massachusetts.

¹R. S. Willey, Nucl. Phys. **40**, 529 (1963).

²L. Lapikas, G. Box, and H. deVries, Nucl. Phys. **A253**, 324 (1975).

³J. Speth and T. Suzuki, Nucl. Phys. **A358**, 139 (1981).

⁴T. Suzuki, H. Hyuga, A. Arima, and K. Yazaki, Nucl. Phys. **A358**, 421 (1981); Phys. Lett. **106B**, 19 (1981).

⁵J. Dubach and W. C. Haxton, Phys. Rev. Lett. **41**, 1453 (1978). Note that the published article contains an error in that the "nucleon resonance" contribution to the exchange current is computed with a wrong sign.

⁶J. Delorme, A. Figureau, and N. Giraud, Phys. Lett. **91B**, 328 (1980).

⁷J. Delorme, A. Figureau, and P. Guichon, Phys. Lett. **99B**, 187 (1981).

⁸H. Toki and W. Weise, Phys. Lett. **92B**, 265 (1980).

⁹M. Haji-Saeid, C. Glasshauser, G. Igo, W. Cornelius, N. Hintz, G. Hoffman, G. Kyle, W. G. Love, A. Scott, and H. A. Theissen, Phys. Rev. Lett. **44**, 1189 (1980).

¹⁰J. R. Comfort, R. E. Segel, G. L. Moake, D. W. Miller, and W. G. Love, Phys. Rev. C **23**, 1858 (1981).

¹¹W. Bertozzi, M. V. Hynes, C. P. Sargent, W. Turchinetz, and C. F. Williamson, Nucl. Instrum. **162**, 211 (1979).

¹²G. A. Peterson, J. B. Flanz, D. V. Webb, H. deVries, and C. F. Williamson, Nucl. Instrum. **160**, 375 (1979).

¹³F. J. Kline, H. Crannell, J. T. O'Brien, J. McCarthy, and R. R. Whitney, Nucl. Phys. **A209**, 381 (1973).

¹⁴R. E. Rand, Nucl. Instrum. **39**, 45 (1966).

¹⁵G. A. Peterson and W. C. Barber, Phys. Rev. **128**, 812 (1962).

- ¹⁶C. W. deJager, H. deVries, and C. deVries, *At. Data Nucl. Data Tables* **14**, 479 (1974).
- ¹⁷R. S. Hicks and S. Jain (unpublished).
- ¹⁸L. Lapikas, A. E. L. Dieperink, and G. Box, *Nucl. Phys.* **A203**, 609 (1973).
- ¹⁹R. S. Hicks, A. Hotta, J. B. Flanz, and H. deVries, *Phys. Rev. C* **21**, 2177 (1980).
- ²⁰F. Borkowski, P. Peuser, G. G. Simon, V. H. Walther, and R. D. Wendling, *Nucl. Phys.* **A222**, 269 (1974).
- ²¹T. W. Donnelly and W. C. Haxton, *At. Data Nucl. Data Tables* **23**, 103 (1979).
- ²²S. T. Tuan, L. E. Wright, and D. S. Onley, *Nucl. Instrum.* **60**, 70 (1968).
- ²³J. Heisenberg, J. S. McCarthy, and I. Sick, *Nucl. Phys.* **A131**, 435 (1970).
- ²⁴R. S. Hicks, *Phys. Rev. C* **25**, 695 (1982).
- ²⁵P. Quentin, private communication.
- ²⁶S. Cohen and D. Kurath, *Nucl. Phys.* **73**, 1 (1965).
- ²⁷J. C. Bergstrom, U. Deutschmann, and R. Neuhausen, *Nucl. Phys.* **A327**, 439 (1979).
- ²⁸G. G. Simon, Ch. Schmitt, F. Borkowski, and V. H. Walther, *Nucl. Phys.* **A333**, 381 (1980).
- ²⁹J. V. Noble, *Phys. Rev. Lett.* **46**, 412 (1981).
- ³⁰H. Uberall, *Electron Scattering from Complex Nuclei* (Academic, New York, 1971), Part A, p. 187.
- ³¹J. Dubach and W. C. Haxton (unpublished).
- ³²T. Suzuki, private communication.
- ³³J. C. Kim, R. S. Hicks, R. Yen, I. P. Auer, H. S. Caplan, and J. C. Bergstrom, *Nucl. Phys.* **A297**, 301 (1978).
- ³⁴B. A. Brown, S. E. Massen, and P. E. Hodgson, *J. Phys. G* **5**, 1655 (1979).
- ³⁵C. K. Lin and L. Zamick, *Nucl. Phys.* **A365**, 411 (1981).
- ³⁶D. Kurath and L. Picman, *Nucl. Phys.* **10**, 313 (1959).
- ³⁷J. C. Bergstrom and R. Neuhausen, private communication.
- ³⁸R. P. Singhal, J. Dubach, R. S. Hicks, R. A. Lindgren, B. Parker, and G. A. Peterson (unpublished).
- ³⁹J. C. Bergstrom, *Nucl. Phys.* **A327**, 458 (1979).